Von Karman Vortices Formation at the Trailing Edge of a Turbine Blade

DANIELE SIMONI, MARINA UBALDI, PIETRO ZUNINO
Department of Fluid Machines, Energy Systems and Transportation
University of Genova
Via Montallegro 1, I-16145 Genova
ITALY
daniele.simoni@unige.it, zunmp@unige.it, pietro.zunino@unige.it

Abstract: - The paper presents the results of an experimental investigation of the von Karman vortices formation at the blade trailing edge of a large scale turbine cascade.
The mean and time varying characteristics of the flow in the trailing edge region were measured by means of a two-component fiber-optic laser Doppler velocimeter over an experimental grid very close to the blade trailing edge. A phase locked ensemble averaging technique has been applied to separate coherent and incoherent contributions in the instantaneous LDV data.
The trailing edge of the central blade of the cascade has been instrumented with a multisensor surface mounted hot-film probe. The probe outputs proportional to the instantaneous wall shear stress were sampled simultaneously with a filtered reference signal from a hot-wire probe located in the wake and sensitive to the vortex periodicity.
Organised periodic structures have been clearly identified in the flow and their evolution in time has been documented through a sequence of instantaneous pictures of the periodic flow field during a cycle of the vortex shedding. Time-averaged and time-resolved ensemble averaged wall shear stresses on the blade trailing edge help to identify the positions where the boundary layers separate and to analyze the effects of the vortex shedding on the wall shear stress along the trailing edge.

Key-Words: - Turbine blade boundary layers, Turbine blade wakes, Von Karman vortices, Wall shear stress, Hot-film measurements.

1 Introduction

Vortex shedding from circular cylinders and aerodynamic bodies has been extensively investigated since the works of von Karman, because it represents a challenging flow problem and an important phenomenon from the applicative point of view, due to the associated dynamic loadings, mechanical vibrations and noise.

Wakes from turbomachinery bladings, as well, present an unsteady character because of the presence of large-scale organised structures arranged in vortex streets. Wakes from cylinders and blades, however, are only apparently similar, because the vortex shedding is greatly influenced by the boundary layer state at the separation point, which depends on the body shape and pressure gradients. The boundary layer development is different for aerodynamic profiles and cylinders and it is also different for the two sides of the high lift profiles of turbomachinery blades.

In the last decade, due to the recognised relevance of the vortex shedding phenomena for turbine blades, an extensive research activity has been performed in the framework of two European Research Projects ("Time varying wake flow characteristics behind flat plates and turbine cascades" and "Turbulence modelling for unsteady flows in axial turbines"), aimed at improving the knowledge of the time-varying turbine wake characteristics [1-5]. Apart from these projects other relevant contributions can be found in literature, including also investigations on turbine bladings operating in transonic regime [6, 7].

Among several significant conclusions and knowledge enhancement, one important finding of the above mentioned investigations was the confirmation, also for turbine wakes, of the hypothesis of Gerrard [8] that the von Karman vortices may originate from the mutual alternating entrainment and the following cut off of the opposite vorticities associated with the two shear

layers formed from the profile boundary layers separating from the opposite sides of the blade trailing edge. This mechanism may also explain the strong dependence of the vortex shedding frequency on the boundary layer state found by Sieverding and Heinemann [9].

Taking into consideration these issues, it appears worth of interest a detailed investigation of the flow in the blade trailing edge region, including the identification of the time-varying locations of the boundary layer separation points on the trailing edge.

To obtain a direct information from the blade surface, the trailing edge region of the central blade of a large scale turbine cascade has been instrumented with an array of surface mounted hot-film sensors which provides output signals proportional to the instantaneous wall shear stress.

The details of the unsteady flow in the region very close to the trailing edge have been investigated by means of a four-beam two-color fibre-optic laser Doppler velocimeter with burst spectrum processors. Ensemble average and triple decomposition of the experimental data provided mean velocity distribution and time evolution of the organised periodic structures embedded in the flow.

2 Experimental Details

2.1 Test facility and instrumentation

The experiment was performed in the DIMSET low speed wind tunnel. The facility is a blow-down continuously operating variable speed tunnel with an open test section of 500x300 mm^2.

The flow was surveyed in the trailing edge region of the central blade of a three-blade large-scale turbine linear cascade. The blade profile is representative of a coolable high pressure gas turbine nozzle blade with a thick trailing edge (D/c=0.053). A three-blade configuration has been selected in order to have larger blade dimensions within the given test section with the purpose of lowering the vortex shedding frequency and increasing the spatial resolution of the measurements. A schematic of the linear cascade is shown in Fig. 1. The main geometrical parameters of the cascade and the test conditions are summarised in Table 1. The coordinates of the blade are given in [1].

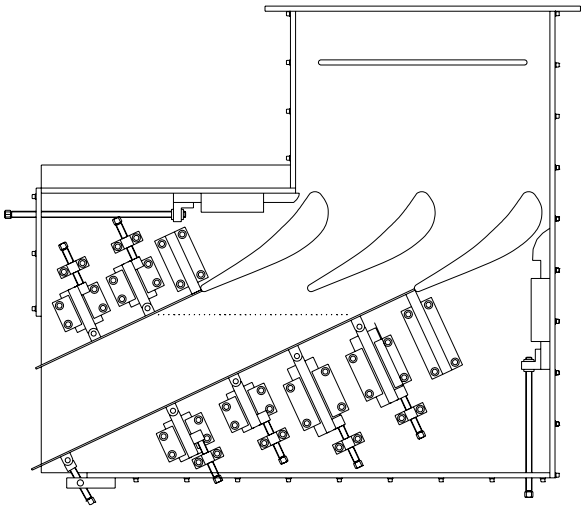

Fig. 1. Test section with the cascade installed

Cascade Geometry	
Chord length	c = 300 mm
Pitch to chord ratio	g/c = 0.7
Aspect ratio	h/c = 1.0
Inlet blade angle	β'_1 = 0°
Gauging angle	β'_2 = 70.9°
Test Conditions	
Relative inlet total pressure	p_{t1} = 3060 Pa
Inlet total temperature	T_{t1} = 293 K
Inlet turbulence intensity	Tu = 1%
Outlet isentropic Mach number	M_{2is} = 0.24
Outlet Reynolds number	Re_c = 1.6·10^6

Table 1. Cascade geometry and test conditions

Two main instruments have been employed or the present investigation: a multisensor surface mounted hot-film probe glued around the trailing edge of the blade at midspan and a four-beam two-colour laser Doppler velocimeter.

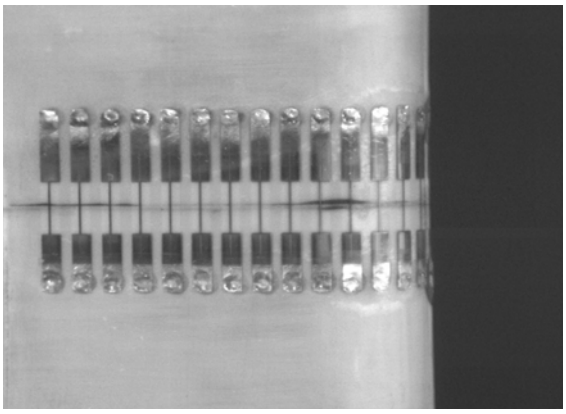

Fig. 2 Hot-film instrumented trailing edge

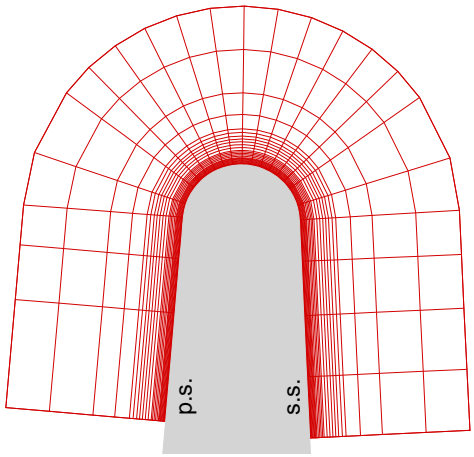

Fig. 3. Experimental domain around the blade trailing edge

The multisensor hot-film probe is obtained by vapour deposition of a thin nickel film, 0.5 μm thickness, on a carrier foil of polyimid, 0.1 mm thick, which is glued on and covers the blade trailing edge region. The probe is made of 30 sensors, 5 mm length and 0.1 mm width, centred on the blade midspan. The distance between each sensor is 2.5 mm, which corresponds to a 18° angular pitch on the trailing edge circle. The hot-film instrumented trailing edge is shown in Fig. 2.

To investigate the flow in the trailing edge region, a four-beam two-colour fibre optic LDV system with back-scatter collection optics (Dantec Fiber Flow) has been used. The light source is a 300 mW argon ion laser operating at 488 nm (blue) and 514.5 nm (green). The probe consists of an optical transducer head equipped with a beam expander (expansion ratio 1.94) connected to the emitting optics and to the photomultipliers by means of optic fibres. The front lens focal length of 310 mm yields, for a 74 mm beam separation, an optical probe volume of 46 μm of diameter and 0.38 mm of length. The probe volume contains two sets of blue and green fringes (with approximate spacing of 2.1 μm and 2.0 μm, respectively), which allow the simultaneous measurement of the two velocity components in the plane perpendicular to the optical axis of the probe. A Bragg cell is used to apply a frequency shift (40 MHz) to one of each pair of beams, allowing resolution of directional ambiguity and reduction of angle bias.

The probe was traversed using a three-axis computer controlled probe traversing system. The motion is transmitted to the carriages by stepping motors through preloaded ball-screw assembly, with a minimum linear translation step of 8 μm.

2.2 Hot-film technique

The surface hot-film sensors are operated using a constant-temperature hot-wire unit, which maintains the film at the selected temperature difference (40°C) with respect to the fluid. The system frequency response, deduced by a square wave test performed with the probe exposed to the flow, was found to exceed 20 kHz. An antialiasing low-pass filter with a cut-off frequency of 20 kHz was applied to the anemometer signal, before it was sampled at a frequency of 50 kHz by means of the 12 bit A/D converter board.

Due to analogy between heat and momentum transfer in boundary layers, the local instantaneous wall shear stress is related to the rate of heat transfer from the hot sensor to the fluid [10].

$$\tau_w = k\left[\left(e^2 - A^2\right)/\Delta T\right]^3 \quad (1)$$

where e is the instantaneous voltage and ΔT *i*s the temperature difference between sensor and fluid.

The calibration of this type of probe is critical but, as was pointed out by several authors (e. g. Hodson [11], Pucher and Göhl [12], Schröder [13]), useful information on the transition and separation phenomena of the boundary layer, as well as on its unsteady properties, can be obtained by a semi-quantitative analysis. The rate of heat transferred to the substrate is proportional to the square of the constant A, and can be approximated by the square of the zero flow voltage e_0^2. Furthermore, if the temperature of the blade is equal to the air temperature, the temperature difference ΔT is proportional to e_0^2 and eq. (1) can be written [11] as

$$\tau_w \equiv k\left[\left(e^2 - e_0^2\right)/e_0^2\right]^3 \quad (2)$$

The hot-film signals were analysed both in the time and in the frequency domains. For each measuring position, a total of 172032 samples was taken.

Phase locked ensemble averages $\tilde{e}$ of each sensor output signal were also obtained with a hot-wire signal used as phase reference of the vortex shedding.

2.3 LDV technique

The unsteady flow in the trailing edge region was surveyed by means of the 2-D LDV probe. The experimental technique has been described in detail in [3] and here will be only briefly outlined. A single sensor hot-wire probe located at a fixed position in the blade wake was used to produce a periodic reference signal at the vortex shedding

frequency, providing an univocal initial time instant for data ensemble average.

The measurements were performed in the mid-span blade-to-blade plane at the nodes of the experimental grid shown in Fig. 3 covering the blade trailing edge region from l/l_{max}=0.88 on the suction side to l/l_{max} = 0.87 on the pressure side. The grid is defined by 24 traverses normal to the blade surface. Seventeen traverses originate from the trailing edge semicircle with a minimum angular pitch of 9° around the trailing edge point. Each traverse is constituted by 29 measuring points. The distance between adjacent points was set at 0.05 mm in the region closest to the wall and was progressively increased in the outer part. The first point was set at a distance of 0.05 mm from the estimated wall position, the last one at 22 mm from the blade surface.

To obtain statistically accurate ensemble averages of the LDV velocities, 50000 validated data for each component have been sampled at each measuring point. Typical data rate values were in the range 500-5000 Hz.

3 Results and Discussion

3.1 Boundary layer characteristics at the blade trailing edge

The time varying characteristics of the blade wake flow are strongly influenced by the boundary layer state at the blade trailing edge (Sieverding and Heinemann [9]). The blade boundary layer development mainly depends on the surface velocity distribution and free stream turbulence. On the pressure side, due to the continuously accelerating flow, in case of natural development, the boundary layer may remain in the laminar-transitional state as far as the trailing edge [14, 15].

A mixed boundary layer condition at the trailing

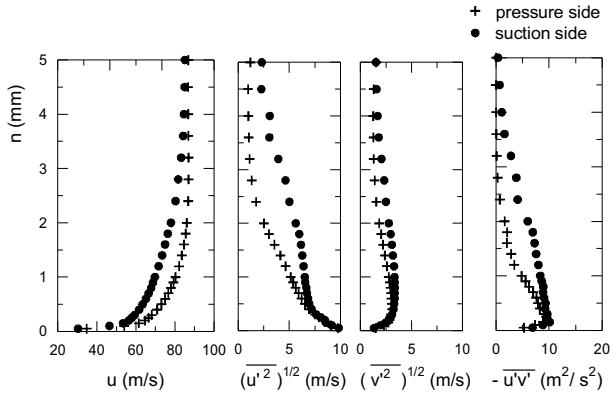

Fig. 4. Boundary layer velocity and turbulence profiles at the blade trailing edge

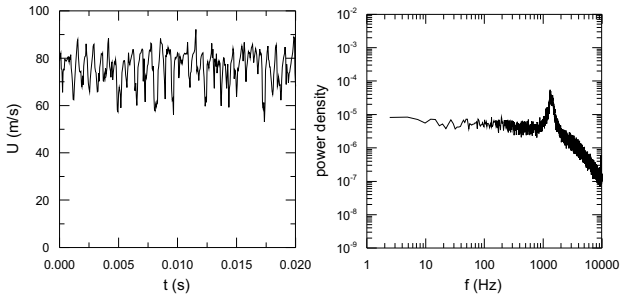

Fig. 5. Instantaneous velocity and power density spectrum in the wake

edge (turbulent boundary layer on the suction side, laminar-transitional on the pressure side) increases the Strouhal number and results in a less symmetrical and stable von Karman street [9]. Therefore, in order to force turbulent conditions on both sides, the pressure side boundary layer was tripped by means of a wire of 0.4 mm diameter located at l/l_{max}=0.78. Suction side boundary layer was extensively investigated in [15, 16]. Boundary layer velocity and turbulence profiles measured just upstream of the trailing edge are shown in Fig. 4. Profiles for both sides are typical of turbulent boundary layers, but on the suction side the thickness is approximately twice that on the pressure side.

Instantaneous velocities were measured in several points in the wake by means of a single sensor hot-wire probe, in order to get a preliminary overview of the time-varying characteristics of the flow. Time traces and power density spectra of the velocity measured at X/D=2.0 and Y/D=-1.0 are given in Fig. 5. The flow in the wake is highly unsteady because of turbulent and organised fluctuations. A peak of energy, corresponding to the vortex shedding frequency, can be easily detected at about 1300 Hz. The corresponding Strouhal number $St = fD/U_2$ is 0.26, in close agreement with the value measured at the VKI on a cascade with the same blade profile and very similar flow conditions [1].

3.2 Time averaged results

To investigate the mechanisms of the vortex formation and the position of the shear layer separation, the trailing edge of the central blade has been instrumented with a multisensor glue-on hot film probe.

The hot-film output $e(t)$ is proportional to the heat transfer from the sensor to the fluid, and hence to the wall shear stress. This signal is, therefore, a good indicator of boundary layer transitions or

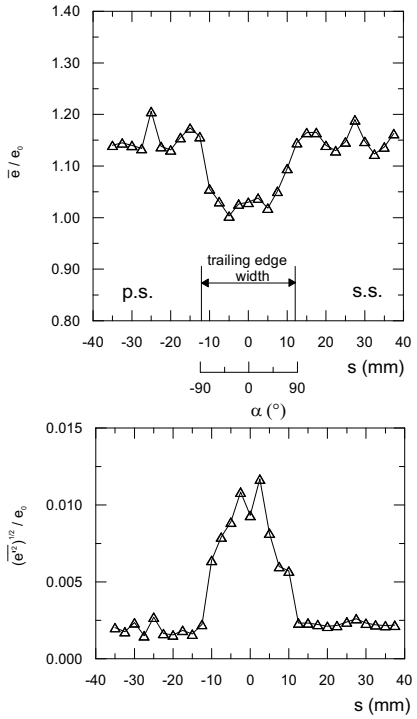

Fig. 6. Time-averaged and rms hot-film signals

separations. To allow a comparative analysis of the different hot-film signals, each hot-film output has been normalised by the corresponding signal e_o obtained in absence of flow.

Figure 6 shows the distributions around the trailing edge of the time averaged and rms hot film signals. The non-dimensional time-averaged signal $\bar{e}/e_0$ drops to 1 in the centre of the trailing edge region, indicating that in the base region the time-averaged wall shear stress tends to zero. The distribution is rather symmetrical.

As the rms values are rather low on the pressure and suction sides of the profile, their strong increase in the trailing edge region is ascribed to the periodic and random unsteadiness associated with the shear layer separations and the vortex shedding phenomenon.

On both trailing edge sides the rms values on the trailing edge corners ($\alpha = \pm 90°$, $s = \pm 12$ mm) are at the lowest level and the unsteadiness starts to increase between these positions and the next sensors ($\alpha = \pm 72°$, $s = \pm 10$ mm).

The large quantity of LDV experimental data acquired allows us to describe in great details the mean flow field in the region immediately adjacent to the blade trailing edge.

The vector plot of Fig. 7 gives an overall view of the development of the time-mean turbulent boundary layers on the two sides of the blade and their separation giving rise to two shear layers and two nearly symmetrical vortices in the corners formed between the separated flow and the trailing edge semicircle. The mean boundary layer separation position can be identified on both sides between 81° and 72° away from the trailing edge central point. These values are in agreement with the 77° value found by Cantwell and Coles [17] for a circular cylinder at high Reynolds number (Re = 140000).

Figure 8 shows the vorticity of the mean flow $\bar{\omega}$ associated with the boundary layer and shear layer development. The suction side boundary layer (negative values) is more extended, but the vorticity associated with the pressure side is more intense.

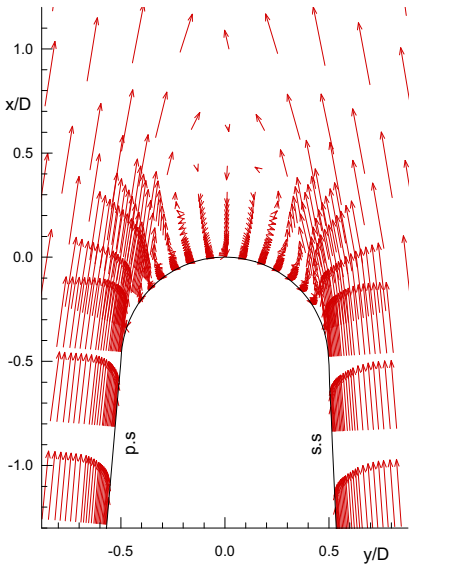

Fig. 7. Vector plot of the time averaged velocity

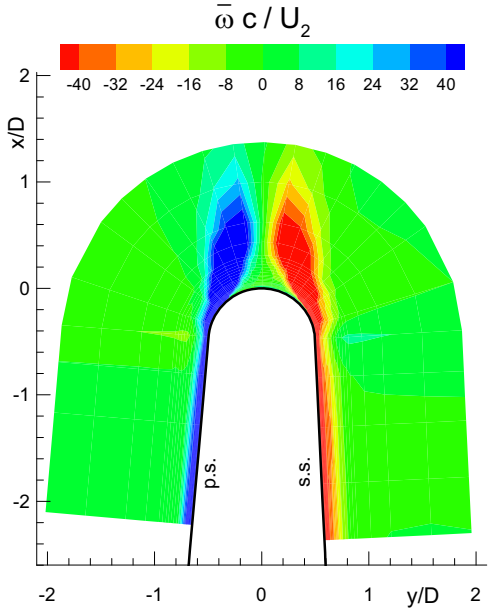

Fig. 8. Vorticity of the mean flow

The distribution presents two elongated cores of opposite high values on the two sides of the wake, which originate in the trailing edge corners from the separating boundary layers. The intensity of the two cores decays rapidly in the streamwise direction. At the downstream boundary of the measuring domain ($x/D \cong 1.4$), the vorticity is reduced to less than 20 per cent of the peak values in the shear layers. Values of the order of 100 for the quantity $\overline{\omega}$ indicate that the local mean vorticity associated with the shear layers is two order of magnitude larger than the mean streamwise acceleration (U_2/c) that the flow undergoes through the cascade.

3.3 Ensemble averaged results

To extract the periodic information from the row data, LDV and the hot-film signals were sampled simultaneously together with a filtered reference signal from a hot-wire probe and an ensemble averaging technique was applied. The hot-wire was located at the periphery of the blade wake, in a region where the velocity field is periodic, with only low turbulence superimposed.

3.3.1 Effect of vortex shedding on blade shear stress

An overall view of the time-space distributions of the phase averaged hot-film outputs is given in Fig. 9. The abscissa is the curvilinear coordinate around the blade trailing edge, the ordinate is the time and the ensemble averaged voltage fluctuations are represented by the colour scale. The phase-averaged results clearly show the periodic nature of the phenomenon on the suction and pressure sides for both boundary layer conditions.

The periodic effect extends upstream of the trailing edge on both pressure and suction sides, but the largest periodic fluctuations take place in the trailing edge region (the extremities of the trailing edge circle are $s = \pm 12$ mm).

It is now important to remind that the quantity represented in the plots is proportional to the periodic fluctuations of the wall shear stress. That means that positive values represent an increase of the wall shear stress associated with the vortex formed in the trailing edge region, while negative values represent a decrease of the wall shear stress. The formation of a vortex behind the blade implies that the flow accelerates near the surface on one side of the trailing edge and decelerates on the other side.

Coming back to the plot of Fig. 9, one can recognize two rows of alternating in time positive and negative nuclei on both trailing edge sides at s=±10 mm ($\alpha = \pm 72°$), that are the points where the boundary layers start to separate according to the time averaged results (Fig. 6). The negative and positive wall shear stress peaks indicate conditions of boundary layer detachment and reattachment which alternate in time and are in phase opposition on the two trailing edge sides.

The other two rows of positive and negative nuclei in the central part of the trailing edge (between s= -5 and s= +5 mm) represent the direct effect of the vortex on the blade surface in the base region. Also this pattern is nearly symmetrical with respect to a line located at the centre of the trailing edge, which represents a discontinuity in the phase angle (phase shift of 180°). That confirms the hypothesis of a periodic formation of nearly symmetrical vortices of opposite vorticity, which alternate in time, in agreement with the alternating detachment of the shear layers from the two sides of the blade trailing edge [3].

3.3.2 The periodic flow in the trailing edge region

The ensemble averaged procedure has been applied also to the LDV data for each measuring point of the experimental domain and the periodic velocity

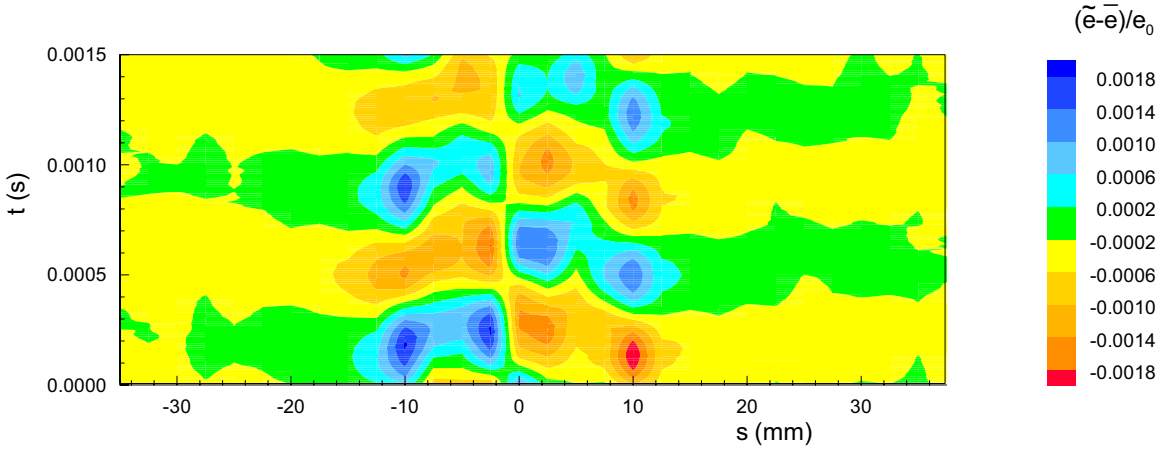

Fig. 9. Time-space distribution of ensemble averaged hot-film signals

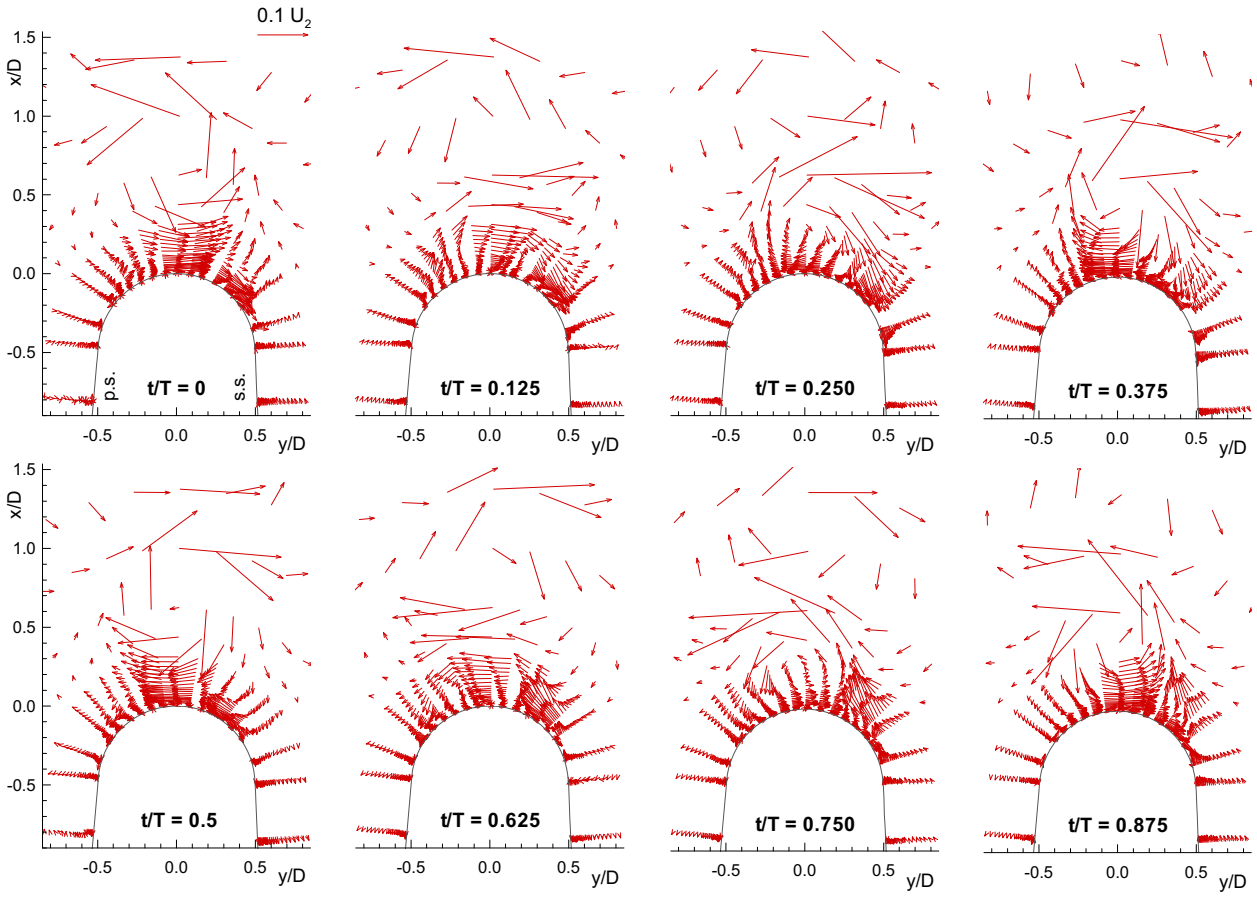

Fig. 10. Vector plots of the periodic flow at eight phases of a vortex shedding cycle

distributions have been interpolated at constant phase. In this way the periodic structures have been extracted from the background flow and the periodic flow field can be represented as a sequence of pictures taken at different phases during a vortex shedding cycle.

Vector plots of Fig. 10 show the periodic velocity field at eight phases during one vortex shedding cycle. An overall view of the vector plots reveals the existence of coherent structures also in the immediate proximity of the trailing edge semicircle. However, the intensity of these organised periodic motions adjacent to the surface is low compared with the periodic flows in the region of interaction of the two shear layers downstream of the mean separated bubble closure point ($x/D > 0.6$). Upstream of the trailing edge semicircle the periodic effect on the boundary layer velocity profiles is in practice irrelevant.

Cicatelli and Sieverding [1] were able to measure the time varying pressure oscillations around the trailing edge of a blade with the same profile adopted for the present experiment. They found that the highest periodic pressure pulsations occur in the region of the boundary layer separation points. The maximum pressure difference over one cycle is about 3 per cent of the downstream dynamic pressure. According to their measurements the induced trailing edge vortex pressure pulsations propagate relatively far upstream. As regards the trailing edge base region, the lack of a dominant vortex shedding frequency did not allow to extract phase-averaged pressure signals.

Recently considerable efforts have been devoted to identify flow coherent structures in turbulent flows (e.g. [18]).

Identification of the organised structures and analysis of their evolution in time can be carried out with the aid of the vorticity of the periodic flow ($\widetilde{\omega} - \overline{\omega}$), shown in Fig. 11, determined taking the curl of the periodic velocity. Starting from $t/T = 0$ a counter clockwise vortex, centred at about $x/D = 0.7$, can be easily identified in both the vector plot of Fig. 10 and in the vorticity distribution of Fig. 11. From $t/T = 0$ to $t/T = 0.25$ the counter clockwise vortex is in the shedding phase. During this phase, flow from the suction side (Fig. 10) feeds the vortex. At the same time cross-stream periodic flow in the separated region, near the trailing edge point, moves from the pressure towards the suction side

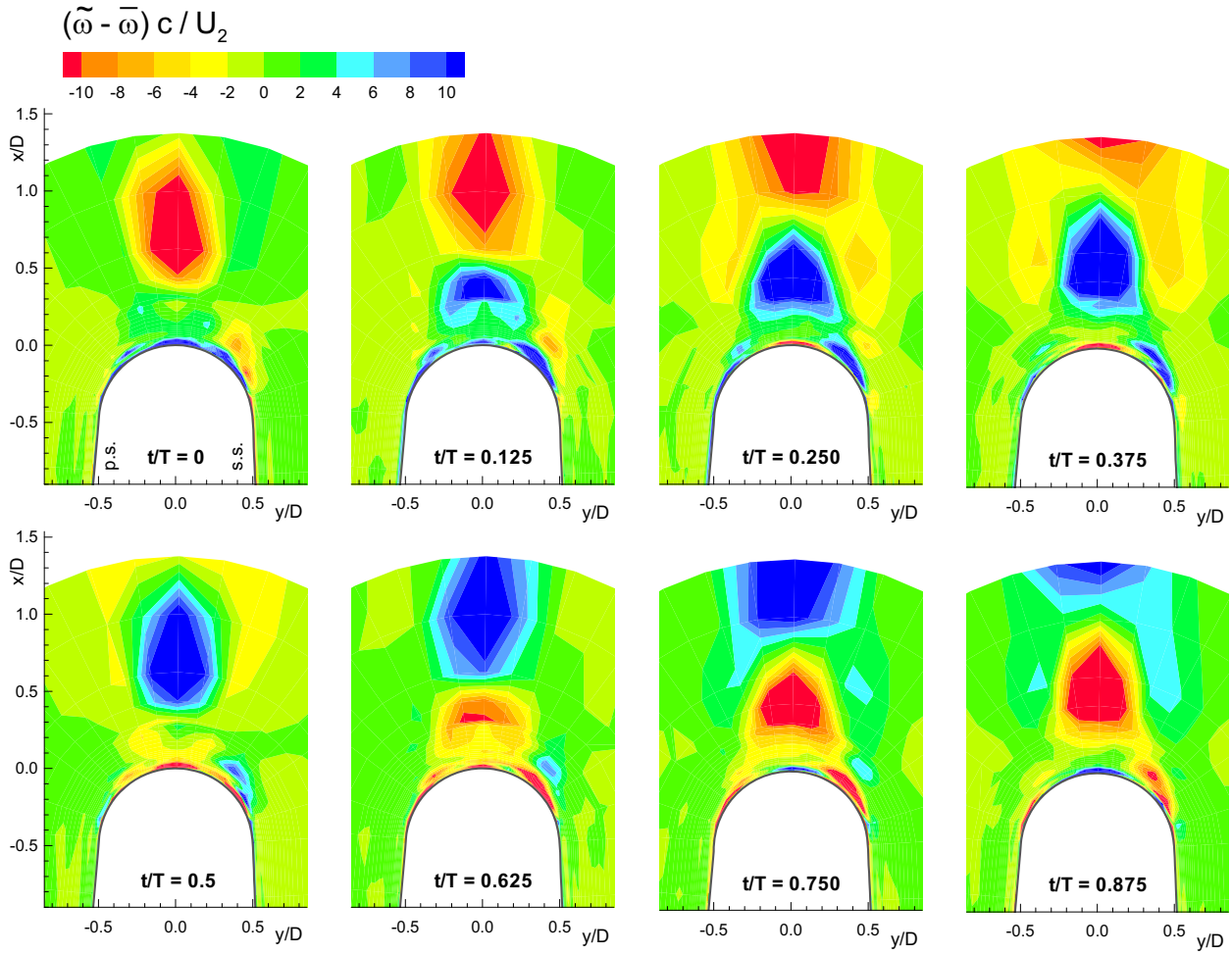

Fig. 11. Instantaneous distributions of periodic flow vorticity at eight phases of a vortex shedding cycle

and, at t/T = 0.125, starts rolling up in a clockwise loop of positive (dark grey) vorticity, which progressively extends in the downstream direction. From t/T = 0.125 to t/T = 0.375, flow from the pressure side enters this new clockwise vortex and, at t/T = 0.375, the cross-flow in the separated bubble, near the trailing edge point, starts to move toward the pressure side, forming the lower branch of the clockwise vortex.

During next phases, from t/T = 0.5 to t/T=0.625, the cross-wise velocity profile adjacent to the trailing edge semicircle is modified giving rise to the new counter clockwise vortex, which develops during the last phases of the period, fed by the suction side periodic flow, and will be shed at the beginning of the following cycle.

4 Conclusions

The signals of a hot-film sensor array mounted around the trailing edge of a blade of a large scale turbine cascade have been analysed to study the effects of vortex shedding on the trailing edge wall shear stress.

Wall shear stress time-varying distributions along the trailing edge show conditions of boundary layer detachment and reattachment which alternate in time with the vortex shedding frequency and are in opposition of phase on the two trailing edge sides.

The region of largest influence of the vortex formation on the wall shear stress is approximately symmetrical around the trailing edge centerline.

Due to the non intrusive nature and directional sensitivity of a fibre-optic two-component laser Doppler velocimeter, the large scale of the model and an accurate automated probe traversing mechanism, a large quantity of experimental data has been produced, which reveals in great detail the mean and periodic characteristics of the flow in the region close to the trailing edge of a turbine cascade. A phase locked ensemble averaging technique developed for separating periodic and random fluctuations and a triple decomposition scheme for the instantaneous velocity have been used to identify periodic organised structures in the flow.

Velocity results are in good agreement with the hot-film data. The profile boundary layers separate from both sides of the trailing edge at angles ranging between 72° and 81° from the trailing edge central point, forming a very short mean separated bubble, with two small vortices located in the corners between the bubble boundary and the trailing edge semicircle. The vorticity associated with the two shear layers is intense, but it decays rapidly in streamwise direction.

Reconstruction of the time evolution of the periodic vector field and the associated periodic vorticity reveals the existence of coherent periodic structures in the trailing edge base region with peaks of opposite vorticity located very close to the wake centerline. The existence of well organised vortical structures in the trailing edge base region does not necessary imply that the vortices are generated in this region, before being shed from the trailing edge. It is possible that these smaller scale periodic motions in phase with the shedding vortex are induced by the vortices formed by interaction of the trailing edge shear layers. However, the trailing edge flow characteristics, like boundary layer separation points, vorticity of the shear layers and separated bubble dimensions influence strongly the shedding mechanism.

Nomenclature

c	blade chord
D	trailing edge diameter
e	hot-film signal
e_0	hot-film signal at zero flow condition
f	frequency
l	surface distance measured from leading edge
l_{max}	surface length from leading to trailing edge
n	normal distance from the wall
s	trailing edge curvilinear coordinate
St	Strouhal number $St = fD/u_2$
t	time
T	period of one vortex shedding cycle
u, v	boundary layer mean velocity components in streamwise and cross-stream directions
u', v'	boundary layer velocity fluctuations in streamwise and cross-stream directions
U	velocity
U_2	cascade outlet velocity
x, y	streamwise and cross-stream direction at the cascade outlet
X, Y	axial and tangential directions at the cascade outlet
α	angular coordinate along the blade trailing edge
ω	vorticity

Superscripts and overbars

‘	fluctuating component
——	time averaged
~	ensemble averaged

References:

[1] G. Cicatelli, C.H. Sieverding, The Effect of Vortex Shedding on the Unsteady Pressure Distribution Around the Trailing Edge of a Turbine Cascade, ASME Paper No. 96-GT-359, 1996.

[2] C.H. Sieverding, G. Cicatelli, J.-M. Desse, M. Meinke, P. Zunino, *Experimental and Numerical Investigation of Time Varying Wakes behind Turbine Blades*, Notes on Numerical Fluid Mechanics, Vol. 67. Vieweg, Braunschweig, 1999.

[3] M. Ubaldi, P. Zunino, An experimental study of the unsteady characteristics of the turbulent wake of a turbine blade, *Experimental Thermal and Fluid Science*, Vol 23, 2000, pp. 23-33.

[4] C.H. Sieverding, H. Richard, J-M Desse, Turbine Blade Trailing Edge Flow Characteristics at High Subsonic Outlet Mach Number, *ASME Journal of Turbomachinery*, Vol. 125, 2003, pp. 298-309.

[5] C.H. Sieverding, D. Ottolia, C. Bagnera, A. Comadoro, J.-F. Brouckaert, J-M Desse, Unsteady Turbine Blade Wake Characteristics, *ASME Journal of Turbomachinery*, Vol. 126, 2004, pp. 551-559.

[6] J.P. Gostelow, M.F. Platzer, W.E. Carscallen, On Vortex Formation in the WakeFlows of Transonic Turbine Blades and Oscillating Airfoils, *ASME Journal of Turbomachinery*, Vol. 128, 2006, pp. 528-535.

[7] E. Göttlich, J. Woisetschläger, P. Pieringer, B. Hampel, F. Heitmeir, Investigation of Vortex Shedding and Wake-Wake Interaction in a Transonic Turbine Stage Using Laser-Doppler-Velocimetry and Particle-Image-Velocimetry, *ASME Journal of Turbomachinery*, Vol. 128, 2006, pp. 178-187.

[8] J.H Gerrard, The Mechanics of the Formation Region of Vortices Behind Bluff Bodies, *Journal Fluid Mechanics,* Vol. 25, Part 2, 1966, pp. 401-413.

[9] C. H. Sieverding, H. Heinemann, The Influence of Boundary Layer State on Vortex Shedding from Flat Plates and Turbine Cascades, ASME Paper No. 89-GT-296, 1989.

[10] B.J. Bellhouse, D. L Schultz, Determination of mean and dynamic skin friction, separation and transition in low-speed flow with a thin-film heated element, *Journal Fluid Mechanics,* Vol. 24, Part 2, 1966, pp. 379-400.

[11] H. P. Hodson, Boundary-Layer Transition and Separation Near the Leading Edge of a High-Speed Turbine Blade, *ASME Journal of Engineering for Gas Turbines and Pow*er, Vol. 107, 1985, pp. 127-134.

[12] P. Pucher, R. Göhl, Experimental Investigation of Boundary *Layer* Separation with Heated Thin-Film Sensors, *ASME Journal of Turbomachinery*, Vol. 109, 1987, pp. 303-309.

[13] Th. Schröder, Investigation of Blade Row Interaction and Boundary Layer Transition Phenomena in a Multistage Aero Engine Low-Pressure Turbine by Measurements with Hot Film-Probes and Surface-Mounted Hot-Film Gauges, *VKI Lecture Series 1991-06*, Bruxelles, 1991.

[14] V. S. Djanali, K.C. Wong, S.W. Armfield, Numerical Simulations of Transition and Separation on a Small Turbine Cascade, *WSEAS Transactionson on Fluid Mechanics*, Vol. 1, 2006, pp. 879-884.

[15] M. Ubaldi, P. Zunino, U. Campora, A. Ghiglione, Detailed velocity and turbulence measurements of the profile boundary layer in a large scale turbine cascade, ASME Paper No. 96-GT-42, 1996.

[16] M. Ubaldi, P. Zunino, Transition and Loss Generation in the Profile Boundary Layer of a Turbine Blade, *WSEAS Transactions on Fluid Mechanics*, Vol. 1, 2006, pp. 779-784.

[17] B. Cantwell, D. Coles, An Experimental Study of Entrainment and Transport in the Turbulent Near Wake of a Circular Cylinder, *Journal Fluid Mechanics*, Vol. 136, 1983, pp. 321-374.

[18] Z. Yang, I.E. Abdalla, On coherent structures in a separated/reattached flow, *WSEAS Transactions on Fluid Mechanics*, Vol. 3, 2008, pp. 143-153.